Design of GaAs Solar Cells Operating Close to the Shockley–Queisser Limit

Xufeng Wang, *Student Member, IEEE*, Mohammad Ryyan Khan, Jeffery L. Gray, *Senior Member, IEEE*, Muhammad Ashraful Alam, *Fellow, IEEE*, and Mark S. Lundstrom, *Fellow, IEEE*

***Abstract*—With recent advances in device design, single-junction GaAs solar cells are approaching their theoretical efficiency limits. Accurate numerical simulation may offer insights that can help close the remaining gap between the practical and theoretical limits. Significant care must be taken, however, to ensure that the simulation is self-consistent and properly comprehends thermodynamic limits. In this paper, we use rigorous photon recycling simulation coupled with carrier transport simulation to identify the dominant loss mechanisms that limit the performance of thin-film GaAs solar cells.**

***Index Terms*—Gallium arsenide, photovoltaic cells, solar energy, thin-film devices.**

I. Introduction

THE efficiency of thin-film single-junction GaAs solar cells has improved substantially over the past several years, reaching impressive efficiencies above 28% [1]–[3]. Despite such a high efficiency, these GaAs solar cells still fall short of the theoretically predicted Shockley–Queisser (SQ) efficiency limit of 33.5% [4], leaving room for additional improvement. This paper is a numerical design study that seeks to clarify the device physics that limits performance of thin-film GaAs solar cells.

As pointed out in [5], recent efficiency gains are correlated with increasing open-circuit voltage $V_{\rm OC}$ arising from reducing radiative recombination $R_{\rm rad}$ by careful design. Specifically, suppression of $R_{\rm rad}$ is achieved by designing the cell to enhance the so-called photon recycling, which can be explained as follows. High-quality GaAs double heterostructures are dominated by radiative recombination, with internal quantum yields of more than 99% [6]. In these thin-film structures, photons emitted by radiative recombination can be reabsorbed (recycled) many times before escaping the cell, thereby effectively increasing the radiative lifetime [7]. The effects of photon recycling were examined by Stern and Woodall [8]; Lush and Lundstrom subsequently proposed to exploit photon recycling in thin-film GaAs solar cells to increase cell performance and decrease material consumption [9]. Martí *et al.* [10] showed that the Shockley diode model is equivalent to the detailed balance model if photon recycling is taken into account. Recent advances in cell design and fabrication exploit photon recycling effects and have brought the efficiency of single-junction thin-film GaAs solar cell close to fundamental limits [1]–[3]. Miller *et al.* have discussed the fundamental processes that limit GaAs solar cell performance from a thermodynamic perspective [4]. Our goal is to do so from a device physics and design perspective and, in the process, to determine the practical limits of cell efficiency.

Numerical simulation is a powerful tool to optimize the design of high-efficiency solar cells [11]. When cells operate near their ultimate efficiency limit, however, care has to be taken to ensure that the simulation is thermodynamically sound. Most numerical simulation codes are not. At $V_{\rm OC}$, photogeneration within the cell is in detail balanced with recombination within the cell. For GaAs, most of the recombination occurs radiatively, but radiative recombination is not a loss, provided that the photon is subsequently reabsorbed within the cell. At $V_{\rm OC}$, in the absence of nonradiative recombination, one photon must leave the cell for every photon that is absorbed. This thermodynamic balance sets the upper limit to solar cell efficiency.

This paper explores practical issues of GaAs solar cells operating near the thermodynamic limit using detailed numerical simulations that include both electrical transport and optics. Electrical transport is well understood. The first step, therefore, is to properly construct a numerical device simulation including photon recycling in a way that is consistent with electrical transport. Our self-consistent electrical–optical model is discussed in Section II. In Section III, we simulate a baseline cell structure as a starting point. Section IV presents a design study, which examines how solar cell device parameters affect performance near the fundamental limit. Insights from the design study suggest a strategy for further efficiency improvement, as discussed in Section V. Our conclusions are summarized in Section VI.

II. Approach

A. Efficiency Limit in Gallium Arsenide Solar Cells

The well-known SQ limit [12] is a material-dependent upper limit to solar cell performance. In practice, nonradiative recombination and other losses reduce the efficiency below this limit. In addition, there is also an upper limit for the effectiveness of light trapping [13], [30]. This light-trapping limit is structure dependent, which means that the upper limit performance of a solar cell is both material and device dependent. In the

Manuscript received July 12, 2012; revised October 26, 2012; accepted December 6, 2012. Date of publication February 8, 2013; date of current version March 18, 2013. This work was supported by Semiconductor Research Corporation Energy Research Initiative Network for Photovoltaic technology.

The authors are with the School of Electrical and Computer Engineering, Purdue University, West Lafayette, IN 47906 USA (e-mail: wang159@purdue.edu; khan23@purdue.edu; grayj@ecn.purdue.edu; alam@ecn.purdue.edu; lundstro@ecn.purdue.edu).

Color versions of one or more of the figures in this paper are available online at http://ieeexplore.ieee.org.

Digital Object Identifier 10.1109/JPHOTOV.2013.2241594

discussion below, we focus on planar cells with an antireflection coating (ARC).

B. Radiative Lifetime Enhancement by Photon Recycling

Photon recycling is a two-step process; photons are first emitted by radiative recombination, and then, a fraction is subsequently reabsorbed (recycled) elsewhere in the device. The net effect is a reduction of the rate of radiative recombination.

Intrinsic radiative recombination (denoted by R_{emit} here) is typically described by the B-coefficient

$$R_{\mathrm{emit}}(\vec{r}) = B\left(np - n_i^2\right) = Bn_i^2\left(e^{q(F_n(\vec{r})-F_p(\vec{r}))/kT} - 1\right) \approx Bn_i^2 e^{q(F_n(\vec{r})-F_p(\vec{r}))/kT} \quad (1)$$

where $F_n(\vec{r})$ and $F_p(\vec{r})$ are position-dependent quasi-Fermi levels for electron and holes respectively. Thus, one straightforward way to incorporate photon-recycling effects in device simulation is to reduce the intrinsic radiative coefficient (or equivalently, enhance the intrinsic radiative lifetime) by reducing B-coefficient according to

$$R_{\mathrm{rad}}(\vec{r}) \equiv R_{\mathrm{emit}} - G_{\mathrm{recycle}} \approx \frac{B}{\phi_r} n_i^2 e^{q(F_n(\vec{r})-F_p(\vec{r}))/kT} \quad (2)$$

where ϕ_r is the so-called photon recycling factor (Asbeck factor [14]), B is the intrinsic radiative recombination coefficient, G_{recycle} is the absorption rate of recycled photons, and R_{rad} is the effective radiative recombination rate as a result of photon recycling.

The limitation of this simple approach is the lack of physically meaningful, well-defined connection between the chosen recycling factor ϕ_r and other parameters such as device geometry and material properties. In addition, the recycling factor has no apparent upper bound to prevent a violation of thermodynamic limit. Thermodynamically, the two steps—intrinsic radiative recombination and recycling of emitted photons—are self-consistently related.

Radiative recombination is an intrinsic property of any material at a finite temperature, and it is related to the absorption coefficient by the Roosbroeck–Shockley equation [15]:

$$R_{\mathrm{emit}}(V=0) = \int_0^\infty R_{\mathrm{emit}}(\nu)d\nu = \int_0^\infty \frac{8\pi\nu^2 n^2}{c^2}\frac{\alpha(\nu)}{e^{h\nu/kt}-1}d\nu \quad (3)$$

where $\alpha(\nu)$ is the optical absorption coefficient at wavelength ν, and n is the index of refraction. The condition $V = 0$ indicates that this equation applies at equilibrium. Away from equilibrium, the quasi-Fermi levels split so that

$$R_{\mathrm{emit}}(\vec{r}) = R_{\mathrm{emit}}(V=0)\, e^{(F_n(\vec{r})-F_p(\vec{r}))/kT}. \quad (4)$$

For thermodynamic consistency of the B-coefficient, (1) and (4) must agree, and therefore

$$B = \frac{8\pi n^2}{n_i^2 c^2}\int_0^\infty \frac{v^2\alpha(\nu)}{e^{h\nu/kt}-1}dv. \quad (5)$$

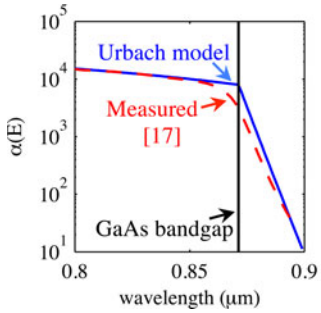

	B coefficient
Urbach model [16]	6.7×10^{-10} /cm^{3}s
Lush [17]	5.0×10^{-10} /cm^{3}s
Varshni [20]	7.2×10^{-10} /cm^{3}s

Fig. 1. Comparison among different intrinsic GaAs absorption coefficients as a function of wavelength close to the GaAs band edge (left graph) and the corresponding effective recombination coefficients (table on right).

The Roosbroeck–Shockley equation connects the electrical radiative recombination and optical absorption coefficient of the material. The B-coefficient is not an independent input, but rather it is determined from absorption coefficients.

Equation (3) is an integral across all wavelengths, but most of the emission occurs in a very narrow wavelength range near the GaAs bandgap. The B-coefficient is closely related to the area under this narrow region, as suggested in (5), so that an accurate knowledge of near band-edge absorption coefficient is essential for quantitative calculation of intrinsic radiative recombination.

Fig. 1 shows a comparison between three sets of intrinsic absorption coefficients: an analytical "Urbach tail" model described in [16], experimental data from [17], and the commonly cited B-coefficient value from [20]. The differences near the bandgap energy translate to an approximate 25% difference in the B-coefficient. The absorption coefficient of GaAs is well known to depend on doping [17], [19]. In this study, we will use the data from [9] which were measured on a 1.3×10^{17} cm^{-3}doped n-type GaAs sample.

After describing radiative emission correctly, the second step in photon recycling involves treating reabsorption of these emitted photons. Photons are emitted isotropically, and ray-tracing methods can be used to trace each emitted ray at each angle and each wavelength in the emission spectrum for each solution node within the device [18].

C. Self-Consistent Photon Recycling With the Semiconductor Equations

In this study, we augment ADEPT 2.0, which solves the semiconductor device equations, by photon recycling based on an approach similar to that of Durbin *et al.* [18]. ADEPT 2.0 is a 1-D self-consistent solar cell simulator capable of simulating layered structures. The simulator is well calibrated, numerically sound, and is available on web [21]. In brief, the solution scheme is as follows.

We begin by calculating the response matrix (see Fig. 2), which quantifies how much absorption occurs at every other node in response to a unit radiative recombination event occurring at a specific node. The optical module traces the isotropically emitted photons from the unit radiative recombination event at every possible angle throughout the structure and determines the absorption at each node. This unit response matrix,

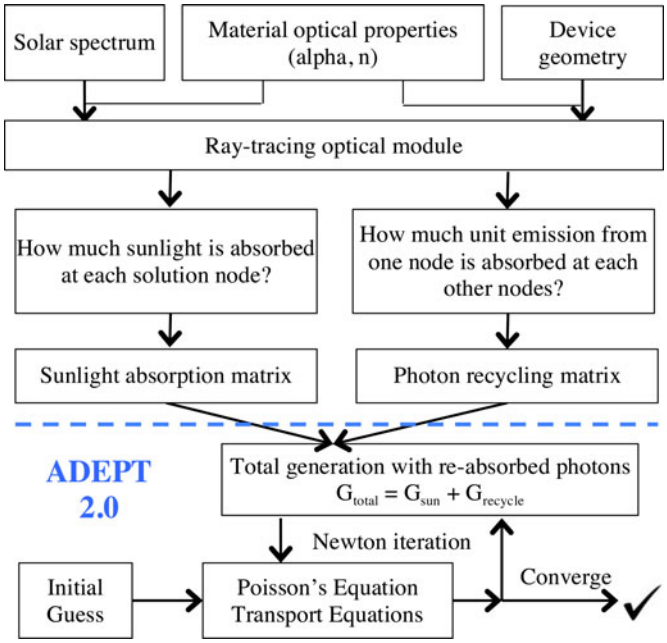

Fig. 2. Overall scheme for ADEPT 2.0 upgraded with the addition of a photon recycling module.

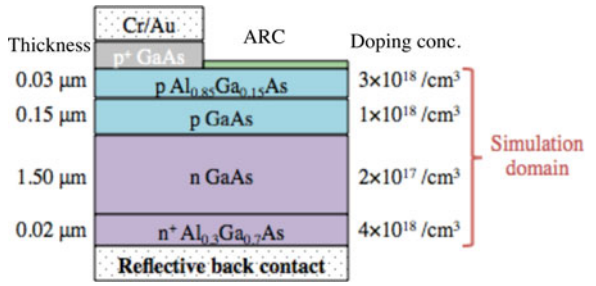

Fig. 3. Idealized single-junction GaAs thin-film solar cell with reflective back contact.

which is termed the "photon recycling matrix," is then passed on to ADEPT 2.0 for the electrical calculation. To ensure consistency, the same ray-tracing module handles the incoming sunlight absorption calculation as well, and the resulting "sunlight absorption matrix" is also passed onto ADEPT 2.0. For a general discussion regarding ray-tracing simulation in solar cells, see [22]. ADEPT 2.0 couples the generation from the two matrices, the electron and hole transport equations, and Poisson's equation into one single Jacobian matrix and uses Newton's method to iterate to the final solution. After each Newton step, R_{emit} is updated with the new local quasi-Fermi level splitting. After obtaining the new R_{emit}, a generation rate due to photon recycling, G_{recycle}, is recalculated. The process continues until convergence is achieved. The model is tested by switching OFF all nonradiative processes and ensuring that the results give the correct thermodynamic upper limit of efficiency.

III. Device Structure

With this thermodynamically consistent model, we can study realistic GaAs solar cells that operate close to the upper limit of efficiency. In this study, we begin with a model structure shown in Fig. 3. In Section IV, we then identify the key loss mechanisms and determine the most important device parameters that limit the efficiency in practice.

The model device is a single-junction GaAs solar cell structure that resembles a recently reported cell [2]. Specifics of the structure in [2] have not been reported; therefore, we make no effort to match experimental data precisely. Our goal here is to use a reasonable device structure and investigate the effects of various key design parameters that affect the performance of these kinds of solar cells.

Fig. 3 summarizes the model cell structure and several key parameters. The structure is typical for single-junction GaAs solar cells by epitaxial liftoff as in [1]. The cell features a heavily doped p-type GaAs thin emitter (0.15 μm) and lightly doped n-type GaAs base (1.5 μm). Two thin high-bandgap-doped AlGaAs layers at front and back form heterojunctions with GaAs, effectively deflecting minority carriers away from contacts to decrease surface recombination. A metallic mirror is placed on the back, which also serves as backside contact. An ARC is typically used on the front to reduce sunlight reflection. For this study, an ARC is not explicitly simulated; therefore, the front reflection loss is summed into shadowing loss, producing a total loss of 6.6%. This percentage was determined by matching the short circuit current reported in [2]. The backside mirror reflectivity was taken from [3].

The escape of photons through the front surface is an important loss mechanism in these cells. The escape cone depends on the ambient index, n, but diffraction effects in the ARC are expected to increase the escape cone somewhat. Photon transport through the ARC is not treated. Instead, we use an ambient index of $n = 1.35$ in an attempt to mimic transmission through the stack of GaAs/ARC (160 nm)/Air by making the front escape cone slightly larger than that of air/GaAs interface. We compared calculations with an ambient index of refraction $n = 1$ to those with $n = 1.35$ and found only a slight increase of 7 mV in V_{OC}, which shows that the specific choice of the ambient index used in modeling has a relatively minor impact compared with the parameters (Shockley–Read–Hall (SRH) lifetime, mirror reflectivity, device width, etc.) we focus on in this paper.

The SRH lifetime (0.5 μs) and the Auger coefficients (7.0×10^{-30}cm^6/s) are reported in [3]. Finally, a series resistance of 0.7 Ω is used to match fill factor (FF) reported in [2]. In our simulation, we have assumed that the perimeter recombination is negligible. Therefore, comparison between theory and experiment is rigorously justified only for GaAs solar cells with passivated edges [23]–[26]. (To first order, edge recombination could be viewed as an effective decrease in bulk SRH recombination lifetime.) With these assumptions, the simulated baseline cell shows performance similar to that of the cell reported in [2] (see Fig. 4).

As discussed in [5], most of the efficiency gain in this thin-film cell, as compared with its substrate counterpart, is achieved through a substantially higher V_{OC}. Fig. 5 shows a comparison of various recombination losses in the device. Radiative

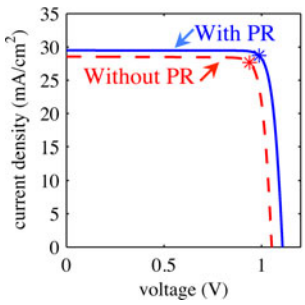

	Baseline (with PR)	Ref. [2]
V_{oc}	1.107 V	1.107 V
J_{sc}	29.49 mA/cm^2	29.47 mA/cm^2
FF	0.867	0.867
Eff.	28.35%	28.3%

Fig. 4. (Left) Baseline light *I–V* characteristics with (blue solid line) versus without (red-dashed line) photon recycling. (Right) The key metrics (V_{oc}, J_{sc}, and FF) obtained for the baseline cell with photon recycling effects (blue solid line on the left) matches those reported in [2] closely.

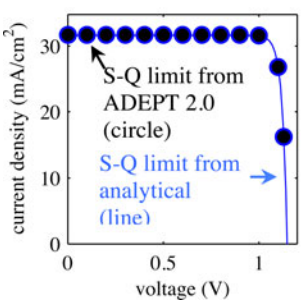

	Shockley-Queisser	Optical Planar
V_{oc}	1.12 V	1.14 V
J_{sc}	33.5 mA/cm^2	31.9 mA/cm^2
FF	0.89	0.89
Eff.	33.5%	32.7%

Fig. 6. (Left) Comparison of *I–V* at the SQ limit by analytical detailed balance method (solid line) and ADEPT 2.0 (black filled circles). (Right) Characteristic parameters for the SQ limit are compared with a planar cell in the table.

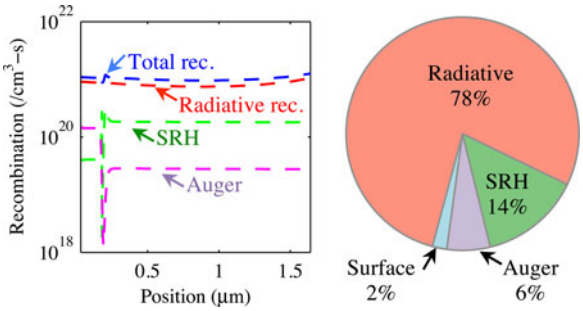

Fig. 5. Radiative, SRH, and Auger recombination within baseline cell at V_{OC}. (a) Recombination rate versus position. (b) Integrated recombination rate at V_{OC} for radiative recombination (Radiative), bulk SRH recombination (SRH), Auger recombination (Auger), and surface SRH recombination (Surface). "Position" on the x-axis corresponds to the depth relative to sun-facing cell surface. Backside mirror is located at the right end of the x-axis. (See Fig. 3.)

recombination (intrinsically emitted minus recycled) dominates throughout (at V_{OC}) the cell structure and is responsible for ~80% of total recombination. The rest is mainly due to SRH recombination. The heterojunction interfaces formed by AlGaAs/GaAs serve as excellent minority carrier mirrors at both the front and back; thus, surface recombination is very low (~2%) and, therefore, not shown in Fig. 5.

IV. Results

With a baseline structure defined, we now proceed to investigate some design parameters and determine the most important loss mechanisms. In this section, we first establish an upper limit for this baseline cell as reference. We then examine the effects of the backside mirror (see Fig. 8), SRH recombination (see Fig. 9), series resistance (see Fig. 10), and cell thickness (see Fig. 11) with respect to the baseline structure to understand how each of these loss factors reduces the cell efficiency from the upper limit.

A. Fundamental Limits

The SQ limit is derived by using detailed balance between absorption of incoming photons from sunlight and radiative emission at cell's temperature described by Planck's law [12], [30]. Since the updated ADEPT 2.0 simulator is thermodynamically consistent, the SQ limit can also be obtained by requiring that all parameters satisfy four SQ conditions: 1) complete absorption, 2) maximum angle entropy [30], 3) no transport bottleneck, and 4) absence of nonradiative recombination.

To ensure that all incident photons with energy higher than GaAs bandgap are completely absorbed at the cell surface, we customize the GaAs absorption coefficient to be artificially high (e.g., 10^7/cm) for energies above GaAs bandgap and zero for those below (step-like). We ensure that the performance of the cell (V_{OC}, J_{SC}, FF) at the thermodynamic limit is insensitive to the exact value of the absorption coefficient.

To ensure the maximum angle entropy implied in the SQ paper, the emission out of the cell must occur at the surface with 2π sr. Therefore, we set the index of refraction for all solar cell layers to be 1 (same as air), effectively making the front escape cone 2π sr to avoid any angle restriction.

To make sure the carriers are collected as soon as they are generated, carrier mobilities are set to very high value (10^8cm^2/V·s. Finally, *all* nonradiative recombination processes (including the fundamental Auger process) are set to zero to be consistent with the SQ assumptions.

Fig. 6 shows the simulated *I–V* from ADEPT 2.0 with the SQ assumptions compared with that obtained from analytical calculation based on detailed balance; the results are identical, as expected. This verifies that the detailed balance model was correctly implemented in the numerical simulation.

We now define the "Optical Planar Limit" by removing the first of the four constrains that define the SQ limit, namely, that of complete absorption. Recall that, in practice, the absorption coefficient in GaAs is finite [9], and therefore, photon absorption in 1.5-μm baseline cell, even with photon recycling, is necessarily imperfect. Therefore, even if the mobilities are presumed infinite and nonradiative, recombination is absent (just as in the SQ analysis), the cell efficiency calculated from ADEPT 2.0 with finite absorption, and photon recycling is still lower than that of the SQ limit.

The table in Fig. 6 compares the SQ limit with the planar optical limit. Although the planar optical limit is lower in efficiency, its V_{OC} is *higher* than that of SQ limit. One can also appreciate this difference in V_{OC} from a detailed balance point of view. The imperfect absorption of the planar cell causes it to have lower absorbance near band edge comparing with the perfectly absorbing cell in the case of SQ limit, as if the planar

cell has a larger bandgap, and thus, a higher $V_{\rm OC}$ results [4]. In this study, we focus exclusively on cells defined by parallel planar surfaces.

B. *Effects of Backside Mirror*

The backside mirror plays an important role in thin-film GaAs solar cells. Traditionally, a metallic backside contact reflects incident sunlight (that is not absorbed in the first pass through the material) back toward the front of the cell to enhance overall absorption and increase $J_{\rm SC}$. In thin-film GaAs solar cells where radiative recombination dominates, it serves another critical role of reflecting *radiatively* emitted photons and contributing to photon recycling.

As discussed in Section II, the emission spectrum peaks around a narrow region near the material's bandgap energy, where the absorption coefficient transitions from high to low. Emitted photons travel several passes within the device before they are reabsorbed, because unless the photons are emitted within the escape cone or absorbed by a nonperfect backside mirror, they are forever trapped within the planar parallel surfaces. Therefore, a radiatively emitted photon within planar device with an incident angle to the planar surface outside of the escape cone will bounce around the structure and eventually be recycled—unless it is absorbed, lost at the backside mirror, or escapes through the edges of the cell. This means a typical photon has to strike the backside mirror several times before it is recycled. As a result, efficiency reductions from a lossy backside mirror are mostly due to a reduction in $V_{\rm OC}$ rather than $J_{\rm SC}$—an important point that is also emphasized in [4].

In the case of a nonperfect backside mirror reflectivity ($< 100\%$), the photons trapped by guiding modes are mostly lost to the mirror after repeatedly striking the backside. The absorption length is about 100 μm for photons having GaAs bandgap energy. For a 1 cm $\times$ 1 cm cell, this translates to an edge-emission affected area of 0.0199 cm^2, which is roughly 2% of the total cell area.

The front escape cone is determined by the difference in the indexes of refraction. This escape cone is $\sim$4% of 2π sr so that $R_{\rm front}\sim$96%. Given the high front reflectivity, the design of back mirror becomes critically important. The back mirror reflectivity used in this study ($R_{\rm back} = 0.85$) is appropriate for a metallic mirror in contact with AlGaAs (see Fig. 3). This reflectivity is higher than that of a mirror exposed in air ($n = 1$) due to the difference in medium indexes. The internal spatial profiles of emission and generation due to photon recycling are complex (see Fig. 7); therefore, we spatially integrate the total. The top part of Fig. 7 plots the ratio of the loss of photons through the back surface to the loss through the front surface as a function of the back mirror reflectivity. The photon loss associated with the backside mirror can be interpreted as an effective escape probability, i.e., the probability of "escape" is proportional to the number of times a photon bounces off the mirror. The losses are seen to be approximately equal when the front and back surfaces have almost the same reflectivity.

Fig. 8 shows the influence of backside mirror reflectivity on $V_{\rm OC}$, $J_{\rm SC}$, and efficiency. As expected, enhancement in backside

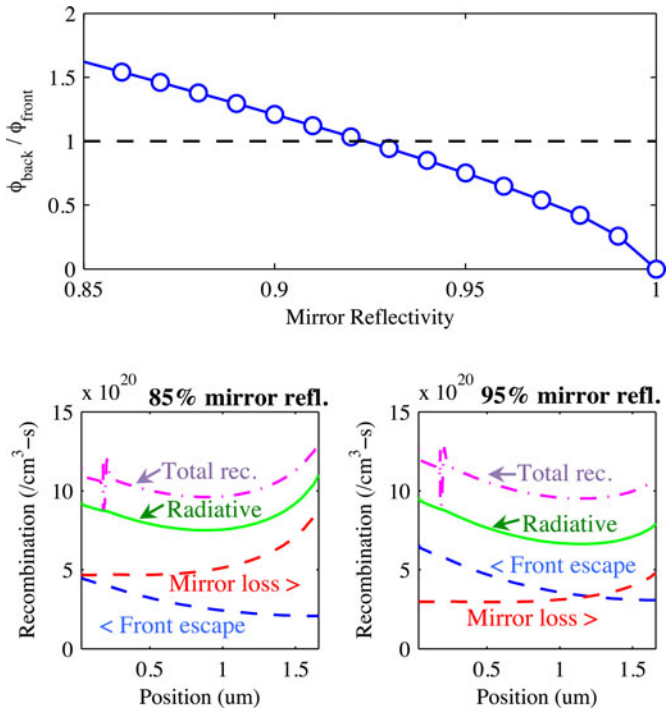

Fig. 7. (Top) Ratio of the loss of photons through the back surface to the loss through the front surface as a function of back mirror reflectivity. (Bottom) For 85% and 95% mirror reflectivity, the percentage of emitted photon escaping from front and losing at backside mirror at different locations within the device under open-circuit condition is shown here. "Position" on the x-axis corresponds to the depth relative to sun-facing cell surface. Backside mirror is located at the right end of the x-axis. (See Fig. 3.)

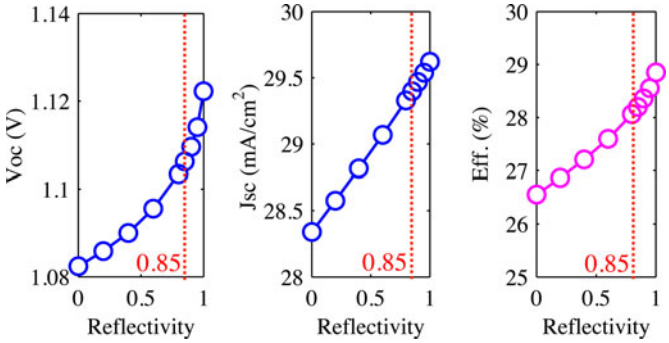

Fig. 8. $V_{\rm OC}$, $J_{\rm SC}$, and efficiency as a function of backside mirror reflectivity. The marked 0.85 reflectivity is used in the baseline case.

mirror reflectivity above $\sim$85% mostly affects the $V_{\rm OC}$. Since GaAs is already a good absorbing material, most of the light is absorbed during the first pass through 1.5-μm base, and backside mirror reflectivity brings minor improvement to $J_{\rm SC}$. Worth noticing is a superlinear improvement on $V_{\rm OC}$ with increasing mirror reflectivity. This is especially true for high-quality mirrors ($>$85%), indicating a substantial opportunity toward higher efficiency. This detailed calculation supports the simpler analysis of [4]. Design of sophisticated mirrors with high reflectivity, however, may not only be nontrivial but expensive as well.

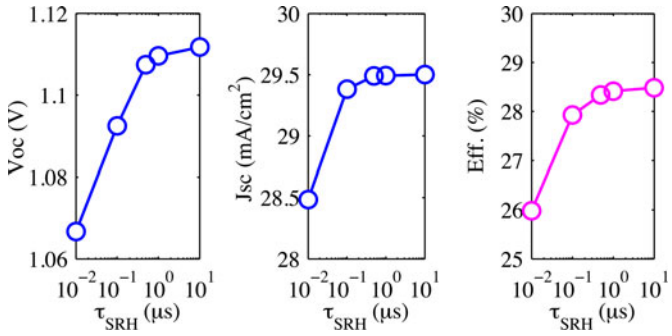

Fig. 9. V_{OC}, J_{SC}, and efficiency as a function of SRH lifetimes. Notice the log scale used on the x-axis.

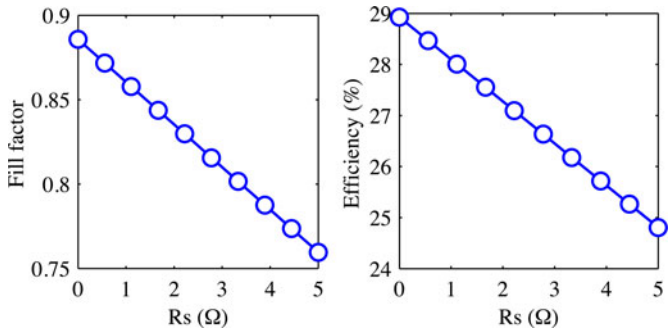

Fig. 10. Fill factor and efficiency as a function of different series resistance values. The cell has an area of 1 cm^2.

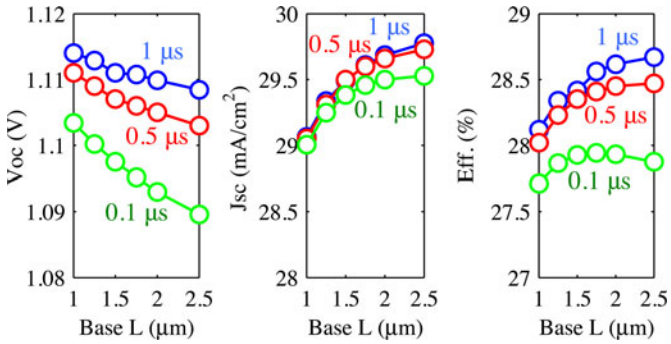

Fig. 11. V_{OC}, J_{SC}, and efficiency as a function of base thickness for three different SRH lifetimes.

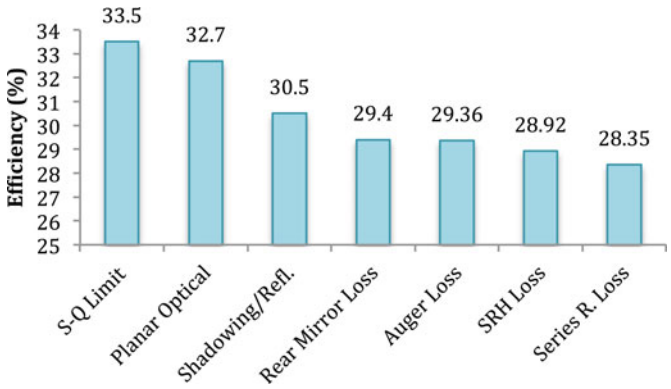

Fig. 12. List of loss mechanisms considered in this study and their impact on baseline cell efficiency.

C. Effects of Shockley–Read–Hall Recombination

Radiative recombination losses can be minimized by photon recycling, but nonradiative recombination, including SRH, Auger, surface recombination, and other losses, will inevitably be present. Auger recombination is a fundamental loss and cannot be avoided, but its effect on cell performance is minimal. SRH recombination, on the other hand, is responsible for ∼20% of all recombination losses with the assumed 0.5-μs lifetime.

Fig. 9 shows how V_{OC}, J_{SC}, and efficiency vary with the SRH lifetime from 0.01 to 10 μs. SRH lifetimes of 1 μs are achievable [9]; therefore, it appears that the SRH lifetime is not a significant limiting factor for further improvement in efficiency. Note that V_{OC}, J_{SC}, and efficiency all saturate for very high SRH lifetime. This is because at high SRH lifetime, radiative recombination becomes the dominant loss mechanism, and cell performance is thus insensitive to further increases of the SRH lifetime.

D. Effects of Series Resistance

Series resistance introduces significant loss in efficiency by lowering the FF. The two most recent reports on record efficiency cells confirmed by the National Renewable Energy Laboratory benefitted mostly from an improvement in FF, while J_{SC} and V_{OC} experienced no major change [2]. This is most likely due to a lowering of series resistance. Fig. 10 shows the impact on FF and efficiency due to different series resistance values. Efficiencies appear to degrade almost linearly (∼1%/Ω) with increasing series resistance.

E. Effects of Base Thickness

One major improvement in single-junction GaAs solar cell comes from the benefits of having a thin base [9]. Compared with a substrate design, a thin film has the advantage of a lower overall recombination region due to a reduction of base thickness and a decrease in radiative recombination since the backside mirror aids in photon recycling.

Any increase in base thickness (see Fig. 11) produces a small increase J_{SC} due to more complete absorption of sunlight. V_{OC}, however, decreases due to a larger volume available for recombination. As a result, the change in overall efficiency is rather small. The detailed impact of base thickness on radiative recombination is related to the backside mirror discussion in Section IV-B. As the base thickness shrinks, emitted photons need to strike the backside mirror more frequently. This significantly increases losses due to the backside mirror. Therefore, there is a tradeoff between more pronounced backside mirror loss and less of a region for radiative recombination to occur—a quantitative connection that only a detailed numerical calculation can precisely capture.

F. Summary of Loss Mechanisms

As a summary of results, Fig. 12 shows a detailed breakdown of efficiency decreases introduced by various loss mechanisms. The chart in this figure is an illustrative way of showing how much the cell efficiency is degraded with each loss

mechanism, starting from the SQ limit on the left. Although this plot is specific to the particular device, and adding the losses in a different order would yield a different efficiency at each step, Fig. 12 serves the purpose of identifying the most important loss factors. The overall efficiency is degraded by a lower $J_{\rm SC}$ due to finite absorption ("SQ Limit" → "Planar Optical"), despite a slightly higher $V_{\rm OC}$ from restriction of emission angles. Efficiency suffers significantly (to 30.5%) by 6% shadowing, front-side sunlight reflection, and any other parasitic losses in the ARC/TCO layers ("Planar Optical" → "Shadowing/Refl"). An imperfect rear mirror with 85% reflectivity further lowers the efficiency by reducing $V_{\rm OC}$ ("Shadowing/Refl." → "Rear Mirror Loss"). Auger recombination is much less significant compared with SRH recombination ("Rear Mirror Loss → "Auger Loss" → "SRH Loss"). In the end, a 0.6 Ω R_S causes further degradation of the efficiency to 28.35% ("SRH Loss" → "Series R. Loss").

V. Discussion

In this paper, we have studied the effects of various design parameters, including SRH recombination, backside mirror reflectivity, series resistance, and cell base thickness, on the practical efficiency limit of single-junction thin-film solar cells. As single-junction GaAs solar cells approach the ultimate limit, critical and controllable parameters have been pushed to be close to best experimentally achievable values so that the gap between the theoretical and experimental limits is reduced.

Not all design parameters can contribute equally in closing the remaining gap. For example, our calculation shows that further improvements in the SRH lifetime or optimization of base thickness would not increase the efficiency significantly. On the other hand, improvements on backside mirror reflectivity beyond 95% will increase the efficiency superlinearly (see Fig. 8); therefore, back mirror reflectivity and series resistances are the two most important parameters on which to focus to create highest efficiency thin-film solar cells.

These conclusions can also be understood by an intuitive argument proposed by Ross [27]. With nonradiative losses such as the backside mirror loss, $V_{\rm OC}$ is degraded from its thermodynamic maximum

$$V_{\rm OC} = V_{\rm OC-max} - kT\ln(k) \tag{6}$$

where k (=1) is the ratio between total recombination and radiative recombination at $V_{\rm OC}$—the inverse of what is known as the external fluorescence efficiency. If backside mirror loss is the dominant nonradiative loss mechanism, its improvement makes the loss term approach zero logarithmically.

Besides the backside mirror, another opportunity to improve efficiency involves lowering series resistance, as seen in Fig. 10. This can be achieved by optimizing the grid design [28]. At the module level, methods such as novel interconnection schemes reducing resistance have also been suggested [29].

Finally, in discussing *practical* efficiency limits, it is important to understand the role of the various uncertainties and assumptions introduced in the simulation. For example, in (5), the choice of the intrinsic carrier concentration n_i influences radiative recombination rate. Since n_i is related to the material bandgap, which is connected to the absorption coefficient, a connection between n_i and optical properties has to be made. This connection is absent at present in our model. Moreover, our choice of ambient index with an effective value of 1.35 is an attempt to model the correct front escape cone. Rigorous optical simulation of the ARC layers with wave effect is needed to accurately model the frequency-dependent transmission and will be a topic of future study.

VI. Conclusion

Designing GaAs solar cells to operate close to the ultimate efficiency limit requires careful device optimization guided by models that accurately incorporate thermodynamic limits. In this paper, we have discussed how to properly simulate solar cells that operate near the thermodynamic limit and have developed a self-consistent device simulator, which includes the thermodynamic limits. In addition, we have conducted a design study that identifies the key loss factors limiting the cell efficiency. We conclude that a good backside mirror and very low series resistance are the most important factors for future improvement in cell efficiency. Nonradiative recombination plays a smaller role as long as the SRH lifetime greater than 0.5 μs can be maintained. Losses due to shadowing and reflection can also be significant but may be difficult to decrease substantially. Therefore, the most promising strategy toward ultimate efficiency for a single-junction GaAs solar cell is to focus on building advanced backside mirrors and developing techniques to achieve very low series resistance.

Acknowledgment

The authors would like to thank Prof. E. Yablonovitch of UC Berkeley and Prof. P. Bermel and J. Wilcox of Purdue University for helpful discussions.

References

[1] B. M. Kayes *et al.*, "27.6% conversion efficiency, a new record for single-junction solar cells under 1 sun illumination," in *Proc. 37th IEEE Photovoltaic Spec. Conf.*, Jun. 2011, pp. 000004–000008.

[2] M. A. Green, K. Emery, Y. Hishikawa, W. Warta, and E. D. Dunlop, "Solar cell efficiency tables (Version 39)," *Progr. Photovoltaics*, vol. 20, no. 1, pp. 12–20, 2012.

[3] G. J. Bauhuis, P. Mulder, E. J. Haverkamp, J. C. C. M. Huijben, and J. J. Schermer, "26.1% thin-film GaAs solar cell using epitaxial lift-off," *Solar Energy Mater. Solar Cells*, vol. 93, pp. 1488–1491, 2009.

[4] O. D. Miller, E. Yablonovitch, and S. R. Kurtz, "Strong internal and external luminescence as solar cells approach the Shockley–Queisser limit," *IEEE J. Photovoltaics*, vol. 2, no. 3, pp. 303–311, Jul. 2012.

[5] H. Atwater, "Paths to high efficiency low-cost photovoltaics," in *Proc. 37th IEEE Photovoltaic Spec. Conf.*, Jun. 2011, pp. 000001–000003.

[6] I. Schnitzer, E. Yablonovitch, C. Caneau, and T. J. Gmitter, "Ultrahigh spontaneous emission quantum efficiency, 99.7% internally and 72% externally, from AlGaAs/GaAs/AlGaAs double heterostructures," *Appl. Phys. Lett.*, vol. 62, no. 2, p. 131, 1993.

[7] J. E. Parrott, "Radiative recombination and photon recycling in photovoltaic solar cells," *Solar Energy Mater. Solar Cells*, vol. 30, pp. 221–231, 1993.

[8] F. Stern and J. M. Woodall, "Photon recycling in semiconductor lasers," *J. Appl. Phys.*, vol. 45, no. 9, pp. 3904–3906, 1974.

[9] G. Lush and M. Lundstrom, "Thin film approaches for high efficiency III-V cells," *Solar Cells*, vol. 30, pp. 337–344, 1991.

[10] A. Martí, J. L. Balenzategui, and R. F. Reyna, "Photon recycling and Shockley's diode equation," *J. Appl. Phys.*, vol. 82, no. 8, p. 4067, 1997.
[11] J. Gray, "The physics of solar cells," in *Handbook of Photovoltaic Science and Engineering*. New York, NY, USA: Wiley, 2011.
[12] W. Shockley and H. J. Queisser, "Detailed balance limit of p-n junction solar cells," *J. Appl. Phys.*, vol. 32, no. 510, p. 510, 1961.
[13] E. Yablonovitch, "Statistical ray optics," *J. Opt. Soc. Amer.*, vol. 72, no. 899, pp. 899–907, 1982.
[14] P. Asbeck, "Self-absorption effects on the radiative lifetime in GaAs–GaAlAs double heterostructures," *J. Appl. Phys.*, vol. 48, pp. 820–822, 1977.
[15] W. van Roosbroeck and W. Shockley, "Photon-radiative recombination of electrons and holes in germanium," *Phys. Rev.*, vol. 94, pp. 1558–1560, 1954.
[16] F. Urbach, "The long-wavelength edge of photographic sensitivity and of the electronic absorption of solids," *Phys. Rev.*, vol. 92, p. 1324, 1953.
[17] G. B. Lush, "Recombination and absorption in n-type gallium arsenide," Ph.D. dissertation, Purdue Univ., West Lafayette, IN [Online]. Available at http://docs.lib.purdue.edu/ dissertations/AAI9301343/, 1992.
[18] S. M. Durbin, J. L. Gray, R. K. Ahrenkiel, and D. H. Levi, "Numerical modeling of the influence of photon recycling on lifetime measurements," in *Proc. 23rd IEEE Photovoltaic Spec. Conf.*, 1993, pp. 628–632.
[19] H. C. Casey, Jr., and F. Stern, "Concentration-dependent absorption and spontaneous emission of heavily doped GaAs," *J. Appl. Phys.*, vol. 47, no. 2, pp. 631–643, 1976.
[20] V. P. Varshni, "Band-to-band radiative recombination in groups IV, VI, and III-V semiconductors," *Phys. Status Solidi*, vol. 19, no. 2, pp. 459–514, 1967.
[21] J. L. Gray, X. Wang, and X. Sun ADEPT 2.0 (2013). [Online]. Available http://nanohub.org/ resources/adeptnpt.
[22] A. W. Smith and A. Rohatgi, "Ray-tracing analysis of the inverted pyramid texturing geometry for high efficiency silicon solar cells," *Solar Energy Mater. Solar Cells*, vol. 29, no. 1, pp. 37–49, 1993.
[23] P. D. DeMoulin, S. P. Tobin, M. S. Lundstrom, M. S. Carpenter, and M. R. Melloch, "Influence of perimeter recombination on high-efficiency GaAs p/n heteroface solar cells," *IEEE Electron Device Lett.*, vol. 9, no. 8, pp. 368–370, Aug. 1988.
[24] T. B. Stellwag, P. E. Dodd, M. S. Carpenter, M. S. Lundstrom, R. F. Pierret, M. R. Melloch, E. Yablonovitch, and T. J. Gmitter, "Effects of perimeter recombination on GaAs-based solar cells," in *Proc. 21st IEEE Eur. Photovoltaic Solar Energy Conf. Exhib.*, 1990, pp. 442–447.
[25] T. B. Stellwag, M. R. Melloch, M. S. Lundstrom, M. S. Carpenter, and R. F. Pierret, "Orientation-dependent perimeter recombination in GaAs diodes," *Appl. Phys. Lett.*, vol. 56, pp. 1658–1660, 1990.
[26] P. E. Dodd, T. B. Stellwag, M. R. Melloch, and M. S. Lundstrom, "Surface and perimeter recombination in GaAs diodes: An experimental and theoretical investigation," *IEEE Trans. Electron Devices*, vol. 38, no. 6, pp. 1253–1261, Jun. 1991.
[27] R. T. Ross, "Some thermodynamics of photochemical systems," *J. Chem. Phys.*, vol. 46, pp. 4590–4593, 1967.
[28] L. Wen, L. Yueqiang, C. Jianjun, C. Yanling, W. Xiaodong, and Y. Fuhua, "Optimization of grid design for solar cells," *J. Semicond.*, vol. 31, p. 014006, 2010.
[29] L. S. Mattos, S. R. Scully, M. Syfu, E. Olson, L. Yang, C. Ling, B. M. Kayes, and G. He, "New module efficiency record: 23.5% under 1-sun illumination using thin-film single-junction GaAs solar cells," in *Proc. 38th IEEE Photovoltaic Spec. Conf.*, 2012, pp. 003187–003190.
[30] M. A. Alam and M. R. Khan, "Fundamentals of PV efficiency interpreted by a two-level model," arXiv:1205.6652v1, May 2012.

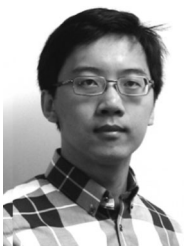

Xufeng Wang (S'08) received the B.S. and M.S. degrees in electrical engineering from Purdue University, West Lafayette, IN, USA, in 2008 and 2010, respectively, where, since 2010, he has been working toward the Ph.D. degree, conducting research with the Network for Photovoltaic Technology.

His current research focuses on the electronic transport and optics coupling in high-performance thin-film solar cells.

Mohammad Ryyan Khan received the B.Sc. degree in electrical and electronic engineering from the Bangladesh University of Engineering and Technology, Dhaka, Bangladesh, in 2009. Since Fall 2009, he has been working toward the Ph.D. degree with Alam Classical and Emerging Electronic Devices Group, School of Electrical and Computer Engineering, Purdue University, West Lafayette, IN, USA.

His research interests include optical designing and modeling of solar cells.

Jeffery L. Gray (SM'11) received the B.S. degree in physics and mathematics from the University of Wisconsin at River Falls, USA, in 1976 and the M.S.E.E. degree in 1978, and the Ph.D. degree in 1982, both from Purdue University, West Lafayette, IN, USA.

He is currently an Associate Professor of electrical and computer engineering and currently serves as the Undergraduate Coordinator for the School of Electrical and Computer Engineering, Purdue University. He specializes in the modeling of photovoltaic devices and systems and has authored or co-authored more than 90 journal and conference papers.

Muhammad Ashraful Alam (M'96–SM'01–F'06) received the B.S.E.E. degree from the Bangladesh University of Engineering and Technology, Dhaka, Bangladesh, in 1988, the M.S. degree from Clarkson University, Potsdam, NY, USA, in 1991, and the Ph.D. degree from Purdue University, Lafayette, IN, USA, in 1994, all in electrical engineering.

He is currently a Professor of electrical and computer engineering with the School of Electrical Engineering and Computer Science, Purdue University, where his research and teaching focus on physics, simulation, characterization, and technology of classical and novel semiconductor devices. From 1995 to 2001, he was with Bell Laboratories, Lucent Technologies, Murray Hill, NJ, USA, as a member of Technical Staff with the Silicon ULSI Research Department. From 2001 to 2003, he was a Distinguished Member of Technical Staff and the Technical Manager of the IC Reliability Group, Agere Systems, Murray Hill. In 2004, he joined Purdue University. He has contributed to more than 150 papers in international journals and has presented many invited and contributed talks at international conferences. His current research interests include stochastic transport theory of oxide reliability, transport in nanonet thin-film transistors, nanobio sensors, and solar cells.

Dr. Alam received the IEEE Kiyo Tomiyasu Award for his contributions to device technology for communication systems. He is a Fellow of the American Physical Society and the American Association for the Advancement of Science.

Mark S. Lundstrom (S'72–M'74–SM'80–F'94) received the B.E.E. and M.S.E.E. degrees from the University of Minnesota, Minneapolis, USA, in 1973 and 1974, respectively, and the Ph.D. degree in electrical engineering from Purdue University, West Lafayette, IN, USA, in 1980.

He is the Don and Carol Scifres Distinguished Professor of Electrical and Computer Engineering with Purdue University, Lafayette, IN, USA. His current research interests focus on the physics of small electronic devices, particularly nanoscale transistors, on carrier transport in semiconductor devices, as well as on devices for energy conversion, storage, and conservation.

Dr. Lundstrom is a Fellow of the American Physical Society and the American Association for the Advancement of Science and a member of the U.S. National Academy of Engineering.